Combining Benzazolo-Oxazolidine Twins toward Multi-state Nonlinear Optical Switches

Quertinmont, Jean; Beaujean, Pierre; Stiennon, Julien; Aidibi, Youssef; Leriche, Philippe; Rodriguez, Vincent; Sanguinet, Lionel; Champagne, Benoît

Published in:
The Journal of Physical Chemistry. B, Condensed matter, materials, surfaces, interfaces & biophysical

DOI:
10.1021/acs.jpcb.1c01962

Publication date:
2021

Document Version
Publisher's PDF, also known as Version of record

THE JOURNAL OF PHYSICAL CHEMISTRY B
A JOURNAL OF THE AMERICAN CHEMICAL SOCIETY

pubs.acs.org/JPCB

Article

Combining Benzazolo-Oxazolidine Twins toward Multi-state Nonlinear Optical Switches

Jean Quertinmont, Pierre Beaujean, Julien Stiennon, Youssef Aidibi, Philippe Leriche, Vincent Rodriguez,* Lionel Sanguinet,* and Benoît Champagne*

Cite This: *J. Phys. Chem. B* 2021, 125, 3918–3931

Read Online

ACCESS | Metrics & More | Article Recommendations | Supporting Information

ABSTRACT: Molecular switches are chemical compounds exhibiting the possibility of reversible transformations between their different forms accompanied by a modification in their properties. Among these, switching of multi-addressable Benzazolo-OXazolidines (BOXs) from a closed form to an open form results in drastic modifications in their linear and nonlinear optical properties. Here, we target molecules containing two identical BOX units (DiBOX) connected by different π-conjugated linkers, and we combine synthesis, UV/visible absorption, and hyper-Rayleigh scattering (HRS) measurements, together with density functional theory (DFT) calculations. Three derivatives have been considered, which differ by the linker: (i) a bithiophene moiety (Bt), (ii) two 3,4-ethylenedioxythiopene (EDOT) units, and (iii) a triad composed of an EDOT−thiophene−EDOT sequence (TtO). As a matter of fact, these systems can adopt three states (CF−CF, POF−POF, and CF−POF) depending on the closed form (CF) or the protonated open form (POF) of each BOX unit. Despite chemical equivalence, stepwise switching of such systems under the addition of a chemical acid or an oxidant has been experimentally evidenced for two of them (DiBOX-Bt and DiBOX-TtO). Then, DFT calculations show that the first BOX opening leads to the formation of a push−pull π-conjugated segment, exhibiting a huge increase in the first hyperpolarizability (β) and a bathochromic shift with respect to the fully closed form. On the contrary, the second BOX opening induces not only a slight bathochromic shift but also a reduction in their β values conferring the great and uncommon abilities to modulate their linear and nonlinear properties over three discrete levels. Among these results, those on DiBOX-Bt agree with the experimental data obtained by HRS measurements and further shed light on their structure−property relationship.

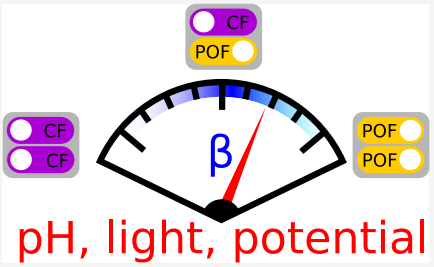

1. INTRODUCTION

Molecular switches constitute a class of compounds that can undergo, under an external stimulation, reversible transformations between at least two metastable states.[1−4] Due to a change in structure, this switching results in variation of molecular properties where the modification of the absorption spectrum, and therefore the color, is certainly one of the most noticeable phenomena. These color changing systems are generally classified according to the nature of the stimulation. Halochromism (also referred to as acidochromism),[5] defining a color change with the pH change, is certainly the most widespread with applications such as pH indicators. Nevertheless, many other chromism phenomena have been reported so far: thermochromism (temperature), photochromism (light irradiation), electrochromism (electrical potential), solvatochromism (solute−solvent interactions), and piezochromism (pressure) to name a few.[6]

These molecular property changes go beyond the absorption spectrum. They can also encompass motion,[7] change of emission (fluorescence and phosphorescence)[8] as in fluorescent proteins, variation of the nonlinear optical responses,[9−11] and modification of the reactivity.

Since the last decade, we and others have shown interest in the modulation of quadratic hyperpolarizabilities where molecular systems based on the **B**enzazolo-**OX**azolidine switchable unit (abbreviated as **BOXs**) have demonstrated remarkable abilities.[12,13] Under stimulation, the oxazolidine ring opening leads to the formation of an indoleninium unit, which acts as a strong electron-withdrawing group (EWG). Combined with an electron-donating group (EDG) through a π-conjugated bridge, the open form of BOXs behaves as a push−pull system providing a drastic enhancement in the first hyperpolarizability (β) and leading to observed high β contrasts between the closed and open forms (Scheme 1). Systems incorporating a BOX unit can switch between two discrete levels, generally denoted as ON and OFF states. Their efficiency (the β contrast) can be maximized by appropriately selecting the EDG and the substituents on the EWG.[14]

Received: March 4, 2021
Revised: March 30, 2021
Published: April 14, 2021

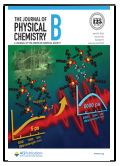

https://doi.org/10.1021/acs.jpcb.1c01962
J. Phys. Chem. B 2021, 125, 3918−3931

Scheme 1. BOX in Its Three Different Forms: CF, OF, and POF[a]

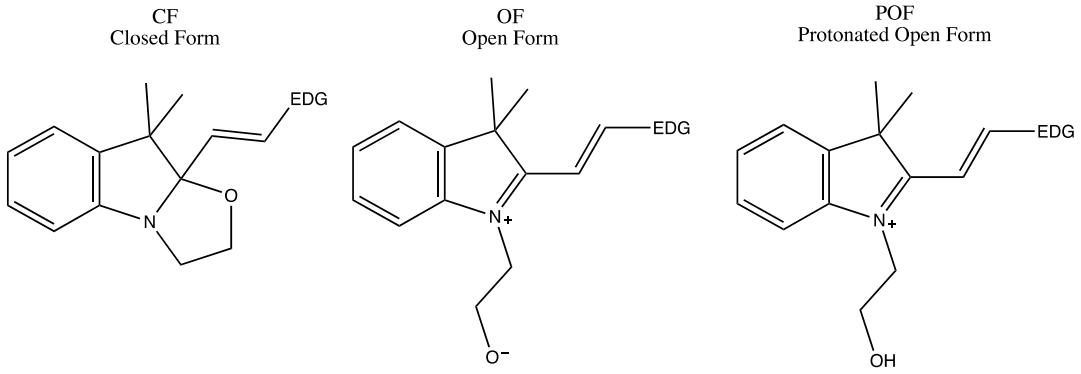

[a]EDG stands for an aromatic fragment with electron-donating characteristic, which could bear different types of substituents.

Scheme 2. Different Levels of Opening of Molecular Switches Combining Two BOX Units, Linked Together by a π-Conjugated Bridge (Top) and the Nature of These Linkers in DiBOX-Bt, DiBOX-BtO, and DiBOX-TtO Compounds (Bottom)

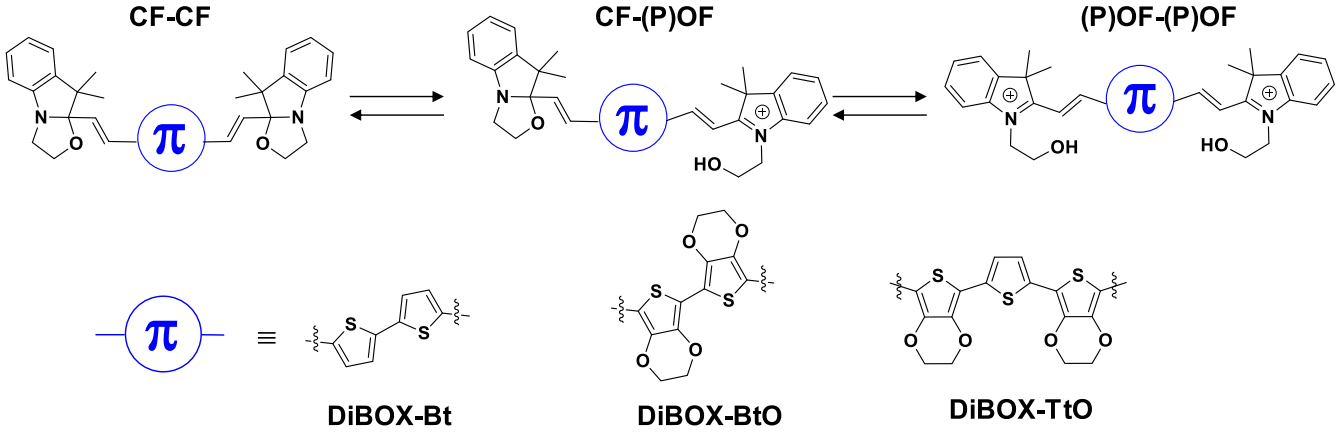

Interestingly, the opening of the oxazolidine ring can be induced by using different kinds of stimulations conferring to BOX's photo-, electro-, and acido-chromic properties.[15] If protonation leads directly to the formation of the positively charged protonated open form (**POF**), UV light irradiation leads to the formation of the metastable zwitterionic open form (**OF**) through cleavage of the C−O bond. In protic media, this later is able to capture a proton to be readily converted into its **POF**. Noticeably, for a given BOX, both open forms (**OF** and **POF**) do not show any difference in their UV/visible (UV/vis) absorption spectra, leading to the conclusion that the state of protonation on the O atom negligibly affects the electronic properties of the molecule. From another point of view, the first excitation energy is not affected by the protonation of the open BOX.[16,17] As a consequence, regeneration of the closed form (**CF**) is generally obtained by treatment with a base or, more rarely, by irradiation with visible light. Besides photochromism and acidochromism, the electrochemical properties of BOXs were investigated recently.[18] In addition to direct oxidation, the oxazolidine ring opening under an electrochemical potential can be obtained by an electromediated process when the BOX unit is associated with a bithiophene moiety as an EDG. The latter is known to form a stable radical cation, which enhances the electrochemical properties of the BOX unit.[14,19] In that case, the assumed mechanism for the opening by oxidation is as follows: (i) oxidation occurs on bithiophene, leading to the formation of a radical-cation species, (ii) first the radical is delocalized to BOX, (iii) then the homolytic cleavage of the C−O bond occurs, and finally (iv) the POF is formed.[15]

To modulate the molecular property over more than two discrete levels, one strategy consists of building units that can switch between more than two states, which can be achieved by using the same triggering mode or not, like dinitrobenzylpyridine[20] and oxazines.[21] In another approach leading to the formation of multi-state molecular switches, several switching units are combined. Therefore, a system combining n different two-state molecular switches exhibits theoretically 2^n different forms, each one possessing its own properties. An illustration is given by the system built from the following three different units: a BOX, a diarylethene, and an alkene linker (which can exhibit two isomers: *cis* and *trans*), leading to an octa-state molecular switch.[22−25] However, in that case, the different reactions of switching can be in competition and may lead to difficulties in controlling one or more forms of the molecular switch, especially if the photoisomerization reactions are achieved in similar conditions. This is particularly true when the different molecular switches are chemically close to each other. Nevertheless, we have recently demonstrated that a stepwise opening selectivity between two identical BOX units is achieved when they are grafted on the same π-conjugated core.[26,27] If such systems did not obey the classical "2^n states" rule, they are able to switch between three different states (**CF−CF**, **POF−CF**, and **POF−POF**) (Scheme 2). As we

https://doi.org/10.1021/acs.jpcb.1c01962
J. Phys. Chem. B 2021, 125, 3918−3931

assessed in this work, from one state to the other, the successive openings of the oxazolidine rings must induce drastic changes in the molecular electronic structures, leading to the first compounds possessing two identical BOX units able to modulate their NLO properties over three discrete levels.

Within this context, molecular switches containing two identical BOX units (denoted as DiBOXs) raise several questions: (i) since the different BOXs are chemically equivalent, is it possible to control the level of opening of these molecules?, (ii) does the chemical nature of the linker affect the selectivity of the successive openings?, and (iii) how does the level of opening of the switch modulate the linear and nonlinear optical properties of these systems? These questions are addressed here by considering three DiBOXs, which differ by the linker connecting the BOX units: the linker of the first compound is composed of a bithiophene (**Bt**), the second one contains two 3,4-ethylenedioxythiopene (EDOT) units (**BtO**), and the last one is composed of an EDOT−thiophene−EDOT sequence (called **TtO**) (Scheme 2). In this way, comparison between DiBOX-Bt and DiBOX-BtO enables to study the impact of a stronger donating π-linker (**BtO**) while comparisons between these and **TtO** tackle the effects of the linker length and π-electron delocalization. These questions are addressed by adopting a multi-disciplinary approach that combines synthesis, experimental characterizations, and quantum chemical calculations. The synthesis of DiBOX-Bt has already been reported together with the control of its successive BOX openings and their impact on the linear optical properties.[26] Depicting the limitation of diBOX system synthesis, we present here the synthesis of diBOX-TtO in our effort to extend the series to more donating π cores. Then, in addition to the characterization of the linear and nonlinear optical properties of both compounds under their different opening states, we present a detailed quantum chemical investigation of their structural, electronic, and optical properties. The latter are performed at the density functional theory (DFT) and time-dependent DFT (TDDFT) levels of approximation.

2. METHODS

2.1. UV/Vis Absorption and Hyper-Rayleigh Scattering Measurements. UV/vis absorption spectra were acquired with a Varian Cary 50 single-beam spectrometer with a 0.1 s integration time every 1 nm. The solvent used is the commercially available spectroscopic grade acetonitrile without further purification. Quartz cuvettes were used with a 1 cm optical path.

The first hyperpolarizabilities were determined by using a homemade setup optimized for polarized HRS measurements[41] and also for polarized third-harmonic scattering of liquids.[42] Briefly, an OPG picosecond laser source (signal: 720−1000 nm, idler: 1150−2200 nm) is used as a probing source to adjust the incident energy (ω) to tune the second-harmonic scattering (2ω). A block power, composed of a half-wave plate and a polarizer, is placed after the source in order to control the incident intensity and deliver the linear vertical polarization. This fundamental relative intensity is precisely determined *via* the measurement of the scattered light intensity by a mirror routed through an optical fiber to a photodiode connected at an oscilloscope. More importantly, the polarization of the incident beam can be continuously controlled (P, S, left/right circular polarization, and all intermediate elliptic polarizations) thanks to the juxtaposition of a half-wave plate and a rotatable quarter-wave plate. This tunability of the incident beam polarization allows us to probe different beta tensor components. The scattered light is collected at 90° and analyzed by a spectrograph using a CCD detector. β_{HRS} of each form of DiBOX-Bt was investigated in acetonitrile solution (varying between 0.25 and 1.0×10^{-4} M) by using the solvent as the internal reference 43. An incident excitation wavelength of 1300 nm has been chosen as a good compromise to avoid both absorption of the fundamental beam from acetonitrile in the near-IR range (ω) and absorption of the scattered harmonic beam (2ω) from the DiBOX samples. The **CF−POF** and **POF−POF** species were obtained from stimulating the **CF−CF** species by adding 1 and 2 equiv of the chemical oxidant, respectively. Figure S6 gathers all the results and shows the variations of the incoherent scattered light at optical frequency 2ω as a function of the concentration of the chromophore and also of the incident power. Then, Figure S7 shows the extracted polarization curves from the different forms. In the case of DiBOX-TtO, the β_{HRS} measurements could not be conducted due to too strong two-photon-induced fluorescence that almost fully hampered the HRS response.

2.2. Theoretical and Computational Aspects. The geometries of all compounds were fully optimized at the DFT level with the M06 XC functional,[44] the 6-311G(d) basis set, and by accounting for solvent effects using the integral equation formalism of the polarizable continuum model (IEF-PCM) (the solvent is acetonitrile).[45] This functional has been selected because it contains an appropriate amount of HF exchange (28%) for predicting the geometry of π-conjugated systems.[46] Real vibrational frequencies demonstrate that the optimized geometries are minima on the potential energy hyper-surface. Since the DiBOX compounds are mostly composed of cyclic units and conjugated segments, the numbers of stable conformers in solution are rather small and the search of those conformers possessing a non-negligible weight within the Maxwell−Boltzmann (MB) statistics can be carried out in a systematic manner. This was done (i) by defining the key torsion angles to distinguish the main conformations (Scheme S1), (ii) by performing rigid scans to locate the extrema of the potential energy hyper-surface, (iii) by combining the minima of the rigid scans to preselect conformations, and then (iv) by performing full geometry optimizations. Finally, only those conformers within an energy window of 12.5 kJ mol^{-1} were kept to calculate the MB populations on the basis of the Gibbs free energies, $\Delta G°$, at 298.15 K. These results are presented in the Supporting Information. This approach is efficient to locate the key conformations because the torsion angles are far enough from each other and, in first approximation, their impact on the total energy is considered as independent from each other, leading to a quasi-additive behavior. Note that, contrary to ref 23, the *cis−trans* isomerizations are not considered here. Indeed, as observed in calculations not detailed here, the fraction of the *cis* form is negligible, so that only the *trans* alkene forms are taken into account.

The vertical excitation energies (ΔE_{ge}) and the transition dipole moments (μ_{ge}) were calculated for at least the 10 lowest-energy excited states at the TDDFT level using the M06-2X XC functional[44] and accounting for solvent effects using the IEF-PCM scheme. The μ_{ge} quantities were used to calculate the oscillator strengths ($f_{ge} = 2/3\Delta E_{ge}\Delta\mu_{ge}^2$) and then employed to plot the UV/vis absorption spectra (each transition was associated with a Gaussian function, centered on

https://doi.org/10.1021/acs.jpcb.1c01962
J. Phys. Chem. B 2021, 125, 3918−3931

ΔE_{ge}, of intensity proportional to f_{ge}, and of full width at half-maximum of 0.3 eV). The differences of dipole moment between the ground and key excited states, $\Delta\mu_{ge} = \mu_e - \mu_g$, were then evaluated. The calculations of all these excited-state-related properties, including μ_e, employ the nonequilibrium solvation approach since electronic excitation processes are very fast with respect to the solvent reorganization.[47] Nonequilibrium solvation TDDFT calculations were performed to evaluate the difference of electronic density between the ground and excited states, $\Delta\rho(\vec{r}) = \rho_e(\vec{r}) - \rho_g(\vec{r})$. Following the procedure described by Le Bahers *et al.*,[48] the barycenters of the positive $[\Delta\rho^+(\vec{r})]$ and negative $[\Delta\rho^-(\vec{r})]$ electronic density variations were evaluated. The distance between these barycenters defines the charge-transfer distance (d_{CT}), while their integration over the whole space gives the amount of charge transferred (q_{CT}). The product of these two quantities gives $\Delta\mu_{ge} = q_{CT} \times d_{CT}$.

The β tensor components were calculated using the TDDFT method[49,50] with the M06-2X XC functional, the 6-311+G(d) basis set, and the IEF-PCM scheme to account for solvent effects. Both static and dynamic (for incident wavelengths of 1907, 1300, and 1064 nm) responses were evaluated. In this work, in parallel to the experimental data, we concentrated on the second harmonic generation (SHG) phenomenon, $\beta(-2\omega;\omega,\omega)$, and more precisely on the hyper-Rayleigh scattering (HRS) first hyperpolarizabilities, $\beta_{HRS}(-2\omega;\omega,\omega)$, and their decompositions.[51] For an experimental setup where the incident light is non-polarized and the vertically polarized (along the z-axis of the laboratory frame) signal scattered at 90° with respect to the propagation direction (y-axis) is detected, the HRS intensity is proportional to the square of $\beta_{HRS}(-2\omega;\omega,\omega)$, which depends on two ensemble averages ($\langle\beta_{ZZZ}^2\rangle$ and $\langle\beta_{ZXX}^2\rangle$) over the molecular orientations

$$\beta_{HRS}(-2\omega;\omega,\omega) = \sqrt{\langle\beta_{ZZZ}^2\rangle + \langle\beta_{ZXX}^2\rangle} = \sqrt{\langle\beta_{ZZZ}^2\rangle\left(1 + \frac{1}{DR}\right)}$$

The depolarization ratio DR, which reflects the chromophore dipolar−octupolar hyperpolarization, is the ratio between the scattered intensities obtained when the incident light is vertically ($\langle\beta_{ZZZ}^2\rangle$) and horizontally ($\langle\beta_{ZXX}^2\rangle$) polarized, respectively. The relationships between these averages (in the laboratory frame) and the molecular tensor components (in the molecular frame) are available from previous papers.[43,52] In the case of a push−pull π-conjugated system, in particular when it is probed close to resonance, the β tensor is often dominated by a single diagonal tensor component (namely, β_{zzz} so that DR = 5 and $\beta_{HRS} = \sqrt{6/35}\beta_{zzz}$). The static β_{HRS} responses were also analyzed in terms of β irreducible spherical representations,[53,54] namely, $|\beta_{J=1}|$, the dipolar contribution, and $|\beta_{J=3}|$, the octupolar one

$$\beta_{HRS}(-2\omega;\omega,\omega) = \sqrt{\frac{10}{45}\left|\beta_{J=1}\right|^2 + \frac{10}{105}\left|\beta_{J=3}\right|^2} = \left|\beta_{J=1}\right|\sqrt{\frac{2}{3}\left(\frac{1}{3} + \frac{1}{7}\rho^2\right)}$$

where $\rho = |\beta_{J=3}|/|\beta_{J=1}|$ is the nonlinear anisotropy factor, describing the relative importance of the octupolar contribution with respect to the dipolar one. Note that ρ and DR are related

$$DR = 9\frac{\left(1 + \frac{2}{7}\rho^2\right)}{\left(1 + \frac{12}{7}\rho^2\right)}$$

For purely dipolar responses, DR = 9 and $\rho = 0$, whereas for the octupolar ones, DR = 1.5 and $\rho = \infty$. For one-dimensional (1D) NLO-phore with a unique dominant diagonal β tensor component, DR = 5 and $\rho = 0.82$.

To visualize the β tensor, the unit sphere representation (USR),[34] was adopted. It consists (i) in computing an effectively induced dipole moment (either static or dynamic like the current SHG responses)

$$\vec{\mu}_{ind} = \overleftrightarrow{\beta} : \vec{E}^2(\theta,\phi)$$

where the tensor nature of β has been evidenced and $\vec{E}(\theta,\phi)$ is a unit vector of electric field, of which the polarization direction is defined in spherical coordinates by the θ and ϕ angles and (ii) by representing all the induced dipole moment vectors on a sphere centered on the center of mass of the compound. This enables highlighting the directions where the second-order polarization is the strongest (it corresponds to the largest induced dipoles), its orientation (the acceptor−donor direction), and subsequently showing how much the β response is dipolar/octupolar. These USRs were plotted using the Drawmol package.[55] All the reported β values are given in a.u. [1a.u. of $\beta = 3.6212 \times 10^{-42}$ m^4 V^{-1} = 3.2064×10^{-53} C^3 m^3 J^{-2} = 8.639×10^{-33} esu] within the T convention.[56]

As noted, a different XC functional was used for calculating the linear and nonlinear optical properties (M06-2X, 54% HF exchange) than the structural and thermodynamic data (M06, 27% HF exchange). This is consistent with previous studies on related compounds,[14] which show that a larger amount of exact Hartree−Fock (HF) exchange is needed to calculate the optical properties.[57−61] All (TD)DFT calculations were carried out using the Gaussian16 package.[62]

3. RESULTS AND DISCUSSION

3.1. Synthesis. The preparation of a few DiBOX compounds has already been reported in the literature. The cornerstone of most of them is the condensation of an aromatic core bearing two carbonyl functions with trimethylindolino-oxazolidine derivatives. If many experimental conditions have been described to perform such condensation (protic/aprotic solvent with and without acid/base catalysis), a recent solvent-free methodology using silica powder[28] has demonstrated high efficiency, allowing the preparation of DiBOX-Bt in good yield.[26] In order to prepare DiBOX-BtO, we have synthesized 5,5′-dicarbaldehyde-2,2′-bis-EDOT (**1**) according to already reported procedures,[29] but replacement of

https://doi.org/10.1021/acs.jpcb.1c01962
J. Phys. Chem. B 2021, 125, 3918−3931

Scheme 3. Preparation of Three DiBOX Derivatives by Solvent-Free Silica-Mediated Condensation between Trimethylindolino[2,1-*b*]oxazolidine and Three Bis-aldehyde Aromatics Prepared by Vilsmeier−Haack Reaction According to the Reported Procedures

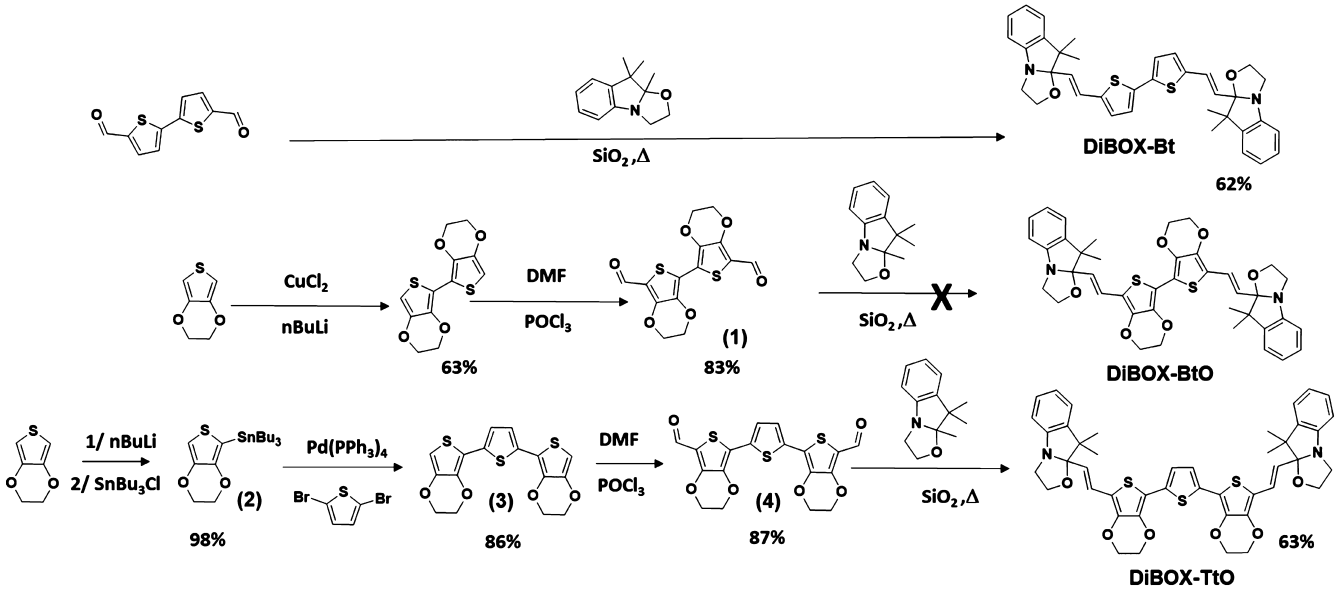

thiophene with EDOT moieties comes with a drop of the solubility of the corresponding bis-aldehyde. Due to this lack of stability, it was impossible to carry out its condensation with 2,3,3-trimethylindolino[2,1,*b*]oxazolidine in classical conditions. Unfortunately, all our attempts to circumvent this problem by changing either the experimental conditions or our synthetic strategy to prepare DiBOX-BtO have been until now unsuccessful. Starting from this, a thiophene was introduced between both EDOT units in order to improve the solubility. A Stille coupling performed on 2,5-dibromothiophene,[30] followed by a classical Vilsmeier−Haack reaction, allowed us to prepare 2,5-di(5′-carbaldehyde-EDOT)thiophene (**4**). Exhibiting a better solubility than **2**, its condensation with 2,3,3-trimethylindolino[2,1,*b*]oxazolidine leading to DiBOX-TtO did not raise any particular problem. Noticeably, it should be mentioned that the higher donor ability of this π-conjugated core, compared to bithiophene, impacts the reaction efficiency as the time of the reaction has to be increased up to 7 h in order to reach a similar yield. All syntheses are resumed in Scheme 3, and more details are provided in the Supporting Information.

3.2. Geometrical Descriptors. The linear and nonlinear optical properties of chromophores can often be analyzed in light of their π-electron conjugation, characterized by simple geometrical quantities, the bond length alternation (BLA), and the torsion or dihedral angles of the π-conjugated segment. Therefore, the geometries of all compounds were fully optimized at the IEF-PCM (acetonitrile)/M06/6-311G(d) level of approximation. For each DiBOX and each of their three states, the Supporting Information provides a summary of the key geometrical parameters (torsion angles and BLAs) of the most stable conformers, their relative Gibbs free energies (ΔG°), their populations with the Maxwell−Boltzmann (MB) approach, and a brief analysis of the optimal torsion angles between the aromatic moieties (Scheme S1 and Tables S1−S9). To describe the π-conjugated segments, instead of one, two types of BLAs were considered: a "global" BLA, taken from one BOX to the other one (denoted as BLA), and "local" BLAs, measured individually on each vinylene bridge (Scheme S1) and denoted as BLA′ and BLA″. For **CF−POF**, the two local BLAs are denoted as BLA′ when associated with the vinylene bridge on the **CF** while BLA″ with the **POF** side. The global BLA values decrease upon the successive openings (Table 1)

$$\text{BLA}[\mathbf{POF{-}POF}] < \text{BLA}[\mathbf{CF{-}POF}] < \text{BLA}[\mathbf{CF{-}CF}]$$

while for the local BLA′ and BLA″, the following trend is observed

$$\text{BLA}''[\mathbf{CF{-}POF}] < \text{BLA}''[\mathbf{POF{-}POF}] \ll \text{BLA}'[\mathbf{CF{-}CF}] \leq \text{BLA}'[\mathbf{CF{-}POF}]$$

Table 1. BLA Values (in Å) for the DiBOXs in Their Different Forms as Evaluated from Geometry Optimizations at the M06/6-311G(d)/IEF-PCM (Acetonitrile) Level of Approximation[a]

		DiBOX-Bt	DiBOX-BtO	DiBOX-TtO
CF−CF	BLA	0.081[b]	0.079	0.072
	BLA′	0.136	0.133	0.133
CF−POF	BLA	0.048	0.041	0.042
	BLA′	0.139	0.136	0.135
	BLA″	0.032	0.013	0.015
POF−POF	BLA	0.032	0.026	0.024
	BLA″	0.049	0.035	0.026

[a]These values are averaged over the MB distributions using the data from Tables S1−S9. [b]All BLA values being negative, their absolute values are reported.

Two trends are evidenced. First, the presence of indoleninium moieties, which correspond to the transformation of a sp^3 C atom into a sp^2 one, increases the general π-electron delocalization (expressed by a smaller BLA). Therefore, a decrease in the excitation energies is expected to come alongside the successive openings. In parallel, opening a BOX strongly reduces the local BLA values (BLA″ ≪ BLA′)

https://doi.org/10.1021/acs.jpcb.1c01962
J. Phys. Chem. B 2021, 125, 3918−3931

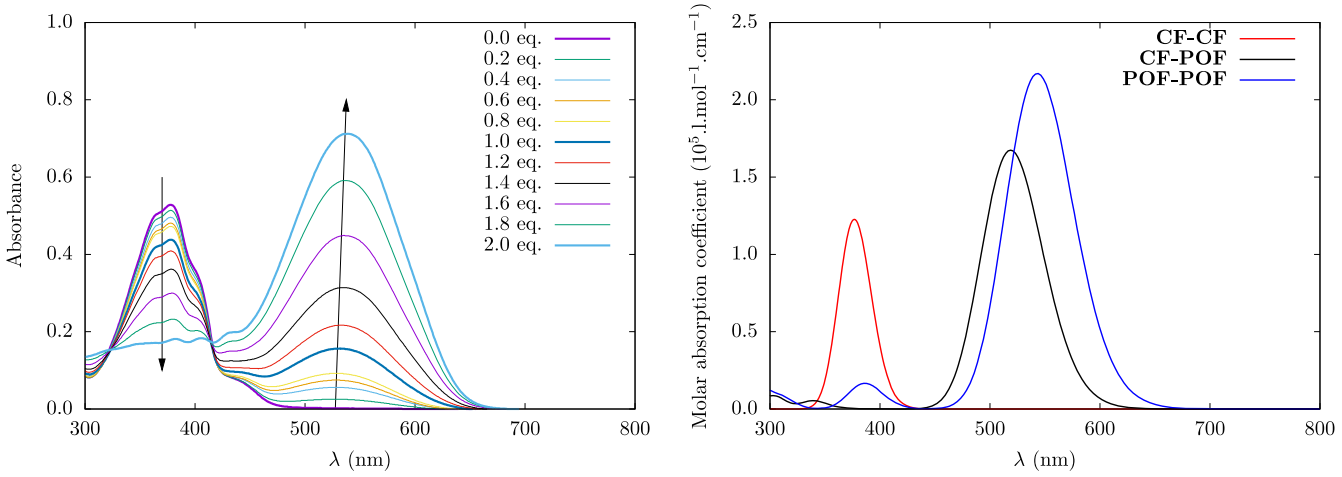

Figure 1. Experimental (left) and simulated (right) UV/vis absorption spectra of DiBOX-Bt. The experimental spectra are obtained in acetonitrile (0.086 mM) along a titration with $NOSbF_6$ as the chemical oxidant. The simulated spectra are given for three different forms (red: **CF−CF**, black: **CF−POF**, and blue: **POF−POF**) using the weighted average results as calculated at the M06-2X/6-311+G(d)/IEF-PCM (acetonitrile) level of theory.

due to the better π-electron delocalization. Noticeably, this transformation of only one BOX unit has an impact on the electron delocalization of both vinylene bridges, as evidenced by a slight increase in BLA′ between **CF−CF** and **CF−POF** forms. Surprisingly, the second BOX opening has antagonistic effects because smaller global BLA values are associated with larger BLA″ for **POF−POF** than **CF−POF** states. These results seem to indicate that the indoleninium−linker delocalization is the strongest when only one BOX is open.

As observed with the status of the BOX unit, the BLA′ values are less affected by the nature of the linker since all BLA′ values range between 0.132 and 0.139 Å. On the other hand, the BLA″ values depend on the nature of the linker: the BLA″ value becomes smaller when the thiophenes are substituted by EDOT. This is due to the ether functions of EDOT, which enhance the delocalization between the linker and the indoleninium(s) by strengthening the donor characteristic of the linker.[31,32] For the DiBOXs in **POF−POF**, the length of the linker has an additional effect on BLA″, which is smaller for DiBOX-TtO than for DIBOX-BtO (0.026 Å *vs* 0.035 Å). This BLA analysis—as well as the differences between the global and local BLAs—finds its roots in the way the successive **CF** openings impact the C−C bond lengths from one BOX to the other (Figure S1). The presence of indoleninium moieties in the π-conjugated system results in a better delocalization, leading to a decrease in BLA. When induced by a single BOX in **POF**, this delocalization attenuates after one aromatic ring. This delocalization is the strongest for the DiBOXs in **CF−POF**, with a stronger weight of the quinoidal form. This effect is then further enhanced by the substitution of a thiophene by an **EDOT**, as illustrated by the variation of BLA″.

3.3. UV/Vis Absorption Spectra and Related Properties. Recording the experimental UV/vis absorption spectra upon stimulation represents certainly the easiest way to monitor the switching abilities of DiBOX-Bt and DiBOX-TtO. As a multi-modal switch, acid or chemical oxidant (generally $NOSbF_6$) aliquots can be generally used in such purpose. However, stimulation by acid is known to be less selective for switching the diBOX system, leading to the coexistence of its three different states. As already performed for DiBOX-Bt,[17−19] the electrochromic behavior of DiBOX-TtO was checked by spectroelectrochemistry experiments (Figure S3), confirming the reversible opening/closing of BOX units under application of an electrochemical potential (at 0.35 and −0.95 V *vs* Fc/Fc^+, respectively). More conveniently, the titration of DiBOX-Bt and DiBOX-TtO with $NOSbF_6$ was monitored by UV/vis spectroscopy (see Methods section for more details). Figures 1 and 2 (with more details in Figures S4 and S5) show that the switching abilities of the DiBOX system are not affected by the nature of the π-conjugated linker. As already reported for DIBOX-Bt, a stepwise transformation of DiBOX-TtO is observed under electrochemical stimulation, leading successively to the **CF−POF** and then the **POF−POF** form from the **CF−CF** form. In both cases, the first BOX opening induces a huge bathochromic shift of the absorption maxima wavelength (151 and 218 nm corresponding to 0.94 and 0.98 eV for DIBOX-Bt and DiBOX-TtO, respectively, Table 2). On the contrary, the second BOX opening induces only a moderate variation of the absorption maxima wavelength (17 and 20 nm corresponding to 0.07 and 0.06 eV for DiBOX-Bt and DiBOX-TtO, respectively). This stepwise switching under external stimulation is translated by an irregular evolution of the UV/vis spectra along the titration with acid or oxidant aliquots. As presented for electrochemical stimulation (Figures 1 and 2), below 1 equiv, two isosbestic points are noticed in each case (321/427 and 368/476 nm for DiBOX-Bt and DiBOX-TtO, respectively). When the stimulation is pushed further, an enhancement of the coloration is observed and, more importantly, this increment did not allow maintaining the observation of the previous isosbestic points, which are replaced by the new ones (326 and 358/464 nm for DiBOX-Bt and DiBOX-TtO, respectively).

Turning now to the QC calculations, using the populations given in the Supporting Information, the weighted averages of the excitation energies were evaluated at the M06-2X/6-311+G(d)/IEF-PCM (acetonitrile) level of approximation. The oscillator strengths were calculated with the objective of simulating the UV/vis absorption spectra (Table 2). The charge-transfer characteristics of the first dominant excitation are also listed. These quantities are useful to interpret the dominant diagonal (in the following expression, along the *z*-

https://doi.org/10.1021/acs.jpcb.1c01962
J. Phys. Chem. B 2021, 125, 3918−3931

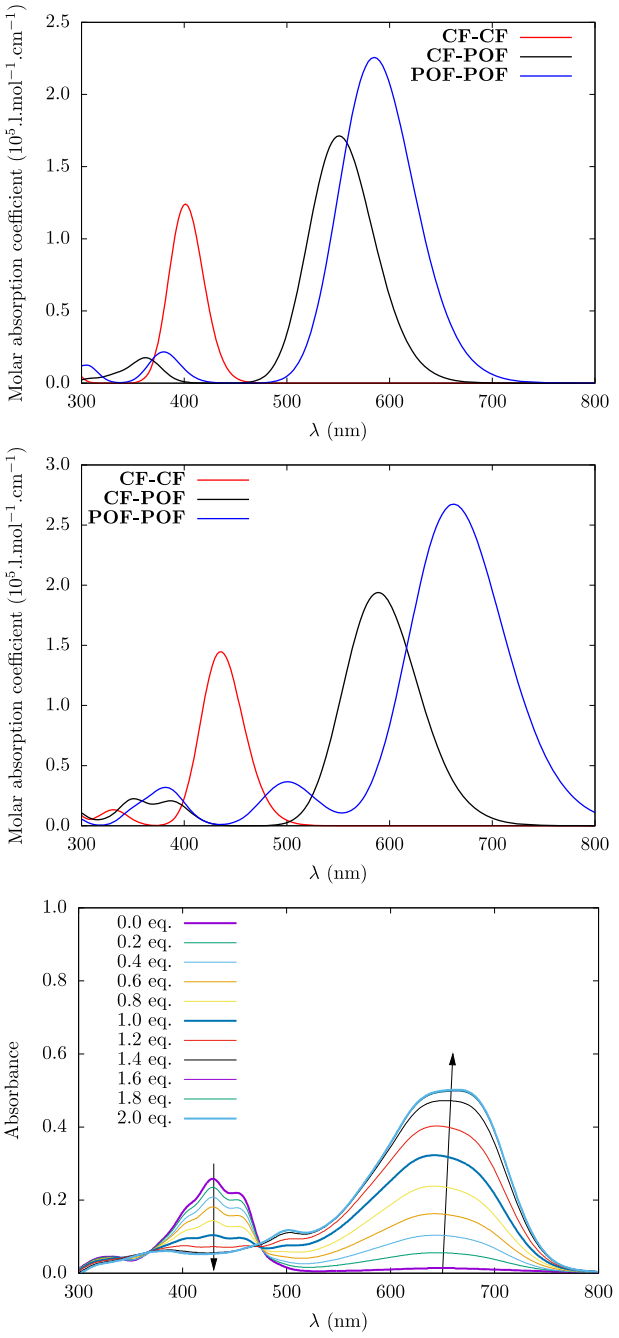

Figure 2. Simulated (top) UV/vis absorption spectra of DiBOX-BtO and comparison between the simulated (middle) and experimental (bottom) UV/vis absorption spectra of DiBOX-TtO. The simulated spectra are given for three different forms (red: **CF−CF**, black: **CF−POF**, and blue: **POF−POF**) using the weighted average results as calculated at the M06-2X/6-311+G(d)/IEF-PCM (acetonitrile) level of theory. The experimental spectra are obtained in acetonitrile (0.06 mM) along a titration with $NOSbF_6$ as the chemical oxidant.

axis) first hyperpolarizability tensor components within the two-state approximation (TSA)[33]

$$\beta_{zzz} = 9\frac{f_{ge}\Delta\mu_{ge}}{\Delta E_{ge}^{3}}$$

As a matter of fact, large β responses can be achieved by (1) a low ΔE_{ge}, (2) a strong absorbance (large oscillator strength, f_{ge}), and (3) a large variation of the dipole moment ($\Delta\mu_{ge}$) between the ground state and the excited state.

The low-excitation energy peak in the UV/vis spectra is attributed to a $S_0 \rightarrow S_1$ excitation. We can notice a good agreement between the experimental maximum wavelengths of absorption and the calculated vertical excitation wavelengths of this first transition (Table 2 and Figures 1 and 2). This substantiates the selection of the M06-2X XC functional for the investigation of the linear optical properties of these systems as a function of the nature of the π-conjugated linker. Numerical simulations confirm that the global evolution of the linear optical properties as a function of the level of opening is not affected by the nature of the linker. In each case, a bathochromic shift accompanies the successive openings (Figures 1 and 2). This shift is more important for the first opening (0.74−0.90 eV) than for the second (0.11−0.23 eV). Still, the value of ΔE_{ge} is strongly influenced by the nature of the linker. By increasing the electron donor characteristic of the π-conjugated linker (vide supra), it is possible to reduce ΔE_{ge}, leading in principle to higher diagonal β tensor components. As a consequence, the substitution of thiophene(s) by EDOT(s) moieties and the enhancement of the linker length result in the smallest ΔE_{ge} values for DiBOX-TtO regardless of the considered form, while DiBOX-BtO presents values in-between the two other compounds.

For the second key parameter in order to reach larger β responses, the evolution of the oscillator strength of the DIBOXs is mainly affected not only by the successive BOX openings but also by the nature of the π-conjugated linker. Indeed, f_{ge} increases by about the same amount (∼0.40−0.60) after each oxazolidine ring opening. For a given form, the absorbance does not vary much between DiBOX-Bt and DiBOX-BtO. On the contrary, the length of the linker affects the oscillator strength: DiBOX-TtO possesses the largest f_{ge} values (∼0.30 higher than DiBOX-Bt and DiBOX-BtO).

Then, achieving large β responses requires a large variation of the dipole moment ($\Delta\mu_{ge}$) between the ground and excited states. This third parameter can be expressed as the product of the charge transfer associated with the (first) excitation, q_{CT}, by its distance d_{CT}. Concerning q_{CT}, the following trend is observed for the three molecules

$$q_{CT}[\text{CF−CF}] < q_{CT}[\text{POF−POF}] < q_{CT}[\text{CF−POF}]$$

q_{CT}[CF−CF] and q_{CT}[POF−POF] do not vary much between the different compounds, between 0.38 and 0.41 e, and between 0.49 and 0.56 e, respectively. Obviously, the q_{CT}[CF−POF] values depend on the nature of the linker and do not fully follow the evolution of electron donor ability of the π-conjugated linker (DiBOX-BtO: 0.49 e, DiBOX-Bt: 0.55 e, and DiBOX-TtO: 0.60 e). Concerning the distance of charge transfer, its evolution is specific to the degree of opening and it depends on the nature of the linker. For DiBOX-Bt, one observes

$$d_{CT}[\text{CF−CF}] < d_{CT}[\text{POF−POF}] \ll d_{CT}[\text{CF−POF}]$$

while for

$$\text{DiBOX-BtO: } d_{CT}[\text{POF−POF}] \sim d_{CT}[\text{CF−CF}] \ll d_{CT}[\text{CF−POF}]$$

and

$$\text{DiBOX-TtO: } d_{CT}[\text{POF−POF}] < d_{CT}[\text{CF−CF}] \ll d_{CT}[\text{CF−POF}]$$

For the three compounds, the **CF−POF** form shows a large d_{CT} value, owing to its push−pull π-conjugated characteristic

https://doi.org/10.1021/acs.jpcb.1c01962
J. Phys. Chem. B 2021, 125, 3918−3931

Table 2. Experimental (Maximum Absorption) Wavelengths (λ_{exp}, nm), Computed (Vertical) Excitation Wavelengths (λ_{ge}, nm), Excitation Energies (ΔE_{ge}, eV), Oscillator Strengths (f_{ge}), Amounts of Charge Transfer (q_{CT}, e), Distances of Charge Transfer (d_{CT}, Å), and Variations of Dipole Moment ($\Delta\mu_{ge}$, D) Associated with the $S_0 \rightarrow S_1$ Excitation of the Three DiBOXs in Their Different Forms as Evaluated at the M06-2X/6-311+G(d)/IEF-PCM (Acetonitrile) Level of Approximation[a]

		λ_{exp}	λ_{ge}	ΔE_{ge}	f_{ge}	q_{CT}	d_{CT}	$\Delta\mu_{ge}$
DiBOX-Bt	**CF−CF**	378[b]	377	3.29	1.39	0.395	0.090	0.176
	CF−POF	529[b]	519	2.39	1.87	0.550	3.287	8.697
	POF−POF	546[b]	543	2.28	2.43	0.494	0.182	0.433
DiBOX-BtO	**POF−POF**	NA	401	3.09	1.38	0.384	0.022	0.040
	CF−POF	NA	551	2.25	1.91	0.498	2.546	6.098
	POF−POF	NA	585	2.12	2.55	0.490	0.020	0.046
DiBOX-TtO	**CF−CF**	428	437	2.84	1.70	0.410	0.425	0.840
	CF−POF	646	589	2.10	2.16	0.601	4.137	11.945
	POF−POF	666	662	1.87	2.98	0.563	0.222	0.600

[a]The averages are weighted using the populations of conformers at 298.15 K. [b]From ref 26.

and the CT character of the lowest energy excitation. Since $\Delta\mu_{ge}$ is the product of q_{CT} by d_{CT} and since d_{CT} is more affected by the level of opening than q_{CT}, the variations of $\Delta\mu_{ge}$ follow those of d_{CT}. The variations of the amplitude of charge transfer between the different DiBOXs and the different forms can be rationalized in terms of the topology of the molecular orbitals implied in the first excitation (Figure 3). For all structures, the first excitation corresponds mostly to a HOMO to LUMO electronic transition. Both frontier orbitals are quite delocalized over the π-conjugated system. For the **CF−CF** form, these orbitals are distributed symmetrically on the linker. For the other symmetric form (**POF−POF**), their distributions extend toward the indoleninium groups, in particular for the HOMO. Finally, for the **CF−POF** form, the distributions are a combination of those of the symmetric forms. Subsequently, the variations of electron density also spread over the molecule (Figure 4), with alternative positive and negative regions, but globally, the electronic charge goes from the linker to oxazolidine, especially when it is open.

Note that for DiBOXs in **CF−CF** and **POF−POF**, the conformation of the linker has a stronger effect on d_{CT} than in **CF−POF**. In these cases, the conformation affects the symmetry of the molecule and modulates the amplitude of d_{CT}. This is particularly true for DIBOX-Bt, where the bithiophene linker can adopt both *syn* and *anti* conformations. The *anti* conformation corresponds to a centrosymmetric structure, resulting in $\Delta\mu_{ge}$ close to zero. On the other hand, the *syn* conformation leads to a structure showing a C_{2v}-like symmetry. As a result, switching from *anti* to *syn* conformation of bithiophene (θ_3: 180° → 0°) results in an increase in the amplitude of $\Delta\mu_{ge}$ (Tables S10 and S12). This effect is further enhanced by the 0° → 180° switching of the θ_2−θ_4 torsion angles. It corresponds to an increase in $\Delta\mu_{ge}$ from 0.056 to 0.451 D for **CF−CF** and from 0.002 to 1.379 D for **POF−POF**. Furthermore, the change of conformation of DIBOX-Bt from *anti* to *syn* in **CF−CF** and **POF−POF** is associated with a reduction in the intensity of the $S_0 \rightarrow S_1$ absorption. For **CF−CF**, the f_{ge} value associated with the $S_0 \rightarrow S_1$ excitation decreases from ∼1.35−1.45 to ∼1.15−1.20, while the f_{ge} value of $S_0 \rightarrow S_2$ is ∼0.30−0.40 when the bithiophene adopts a *syn* conformation. For **POF−POF**, the θ_2−θ_4 torsion angles also impact the f_{ge} of the two first excitations. For the second excitation, conformer 6 (θ_2 and θ_4: s-*cis*) has f_{ge} = 0.12, conformer 4 (θ_2: s-*trans* and θ_2: s-*cis*) has f_{ge} = 0.39, and conformer 2 (θ_2 and θ_4: s-*trans*) has f_{ge} = 0.77. For the form with the largest oscillator strength associated with the second excitation (**POF−POF-2**), this excitation was further analyzed. ΔE_{ge} is 1 eV larger than for the first excitation (3.22 eV *vs* 2.28 eV), the oscillator strength is relatively weak (0.77 *vs* 2.42), still

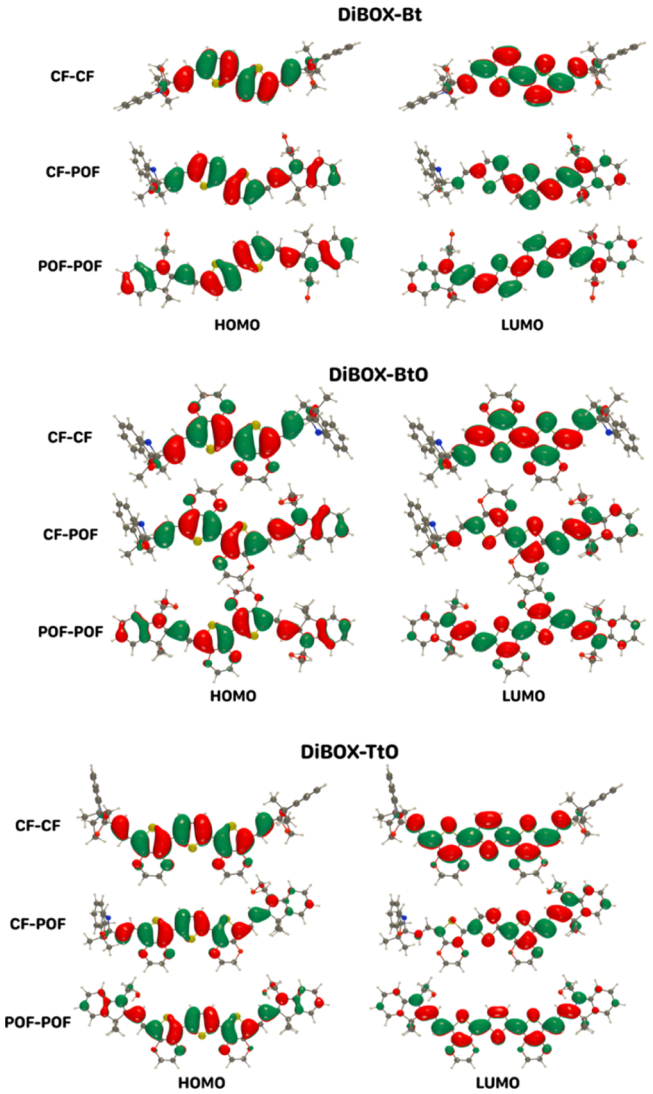

Figure 3. HOMO and LUMO of DiBOXs (in their most stable conformations), which mostly determine the first excitation of these compounds as evaluated at the M06-2X/6-311+G(d)/IEF-PCM (acetonitrile) level of theory. Green = negative, red = positive, and isovalue = 0.02 a.u.

https://doi.org/10.1021/acs.jpcb.1c01962
J. Phys. Chem. B 2021, 125, 3918−3931

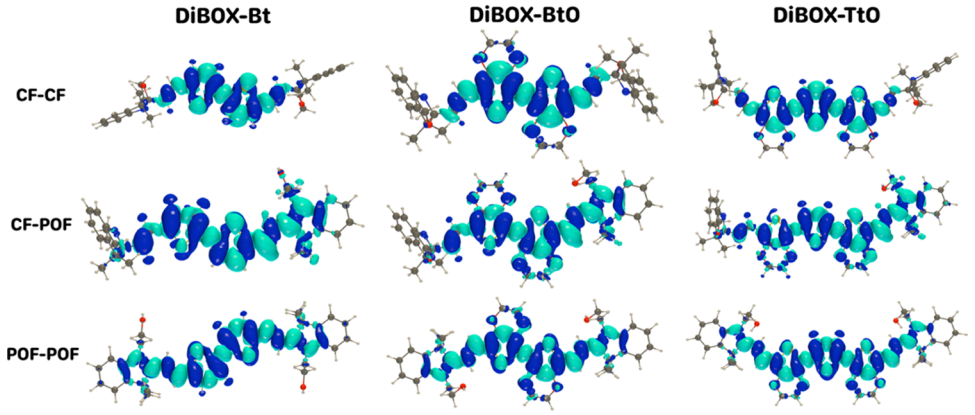

Figure 4. Variation of electron density associated with the first excitation for the three DiBOXs (in their most stable conformations) as evaluated at the M06-2X/6-311+G(d)/IEF-PCM (acetonitrile) level of approximation. Cyan: positive, blue: negative, and isovalue: 0.0004 a.u.

Table 3. β_{HRS} Values (10^3 a.u., Static and Dynamic Fields at λ = 1907, 1300, and 1064 nm) and Static β_{ZZZ}, β_{ZXX}, $|\beta_{J=1}|$, $|\beta_{J=3}|$ (10^3 a.u.), DR, and ρ for the DiBOXs in Their Different Forms as Evaluated at the TDDFT/M06-2X/6-311+G(d)/IEF-PCM (Acetonitrile) Level of Theory[a]

		β_{HRS}				exp.
		Inf.	1907 nm	1300 nm	1064 nm	1300 nm
DiBOX-Bt	CF−CF	0.4	0.3	0.4	0.5	4.1 ± 0.2 (2.49)
	CF−POF	35.9	33.4	77.1	734.3	88.3 ± 4.5 (4.01)
	POF−POF	9.6	6.7	11.1	39.0	47.3 ± 2.4 (2.74)
DiBOX-BtO	CF−CF	1.3	1.2	1.7	2.6	
	CF−POF	37.4	33.4	92.8	433.8	
	POF−POF	0.3	0.3	1.2	1.6	
DiBOX-TtO	CF−CF	2.1	1.8	2.7	4.7	
	CF−POF	80.6	87.5	391.8	415.3	
	POF−POF	9.0	9.0	48.5	40.6	
		β_{ZZZ}	β_{ZXX}	DR	$\|\beta_{J=1}\|$	$\|\beta_{J=3}\|$	ρ
		static values					
DiBOX-Bt	CF−CF	0.4	0.2	3.54	0.6	0.8	1.25
	CF−POF	32.6	14.9	4.79	66.2	57.2	0.86
	POF−POF	8.5	4.4	3.74	15.8	18.5	1.17
DiBOX-BtO	CF−CF	1.2	0.5	4.98	2.5	2.0	0.82
	CF−POF	34.0	15.7	4.67	68.5	61.2	0.89
	POF−POF	0.3	0.2	2.31	0.4	0.9	2.20
DiBOX-TtO	CF−CF	1.9	0.9	4.56	3.8	3.5	0.92
	CF−POF	73.4	33.3	4.84	149.3	127.2	0.85
	POF−POF	7.6	4.7	2.61	12.2	22.3	1.83

[a]These are averaged values calculated using the Boltzmann populations at 298.15 K. The last column reports experimental data at 1300 nm (DRs are given under parentheses).

its $\Delta\mu_{ge}$ is relatively high for this considered conformer (0.62 D), leading to a small but non-negligible contribution to β (this conformer represents 18.5% of the total population at 298.15 K).

For DiBOX-BtO, the two EDOT units adopt an *anti* conformation due to the repulsion between these units, resulting in a small $\Delta\mu_{ge}$ value, especially for **CF−CF** (between 0.04 and 0.05 D) and **POF−POF** (between 0.03 and 0.12 D) (Tables S13 and S14). Since the linker of DiBOX-TtO possesses three thiophene-based units, it cannot show a centrosymmetric structure. The **CF−CF** and **POF−POF** forms correspond to Λ-shaped NLO-phores with a C_{2v}-like symmetry. The displacement of the electron cloud occurring along the first excitation is a displacement from the center of the linker to the BOX moieties. The amplitude of d_{CT} (and $\Delta\mu_{ge}$) is enhanced by constraining the linker, for example, switching from *anti* to *syn* conformation between the thiophene-based units (θ_3−θ_4: 180° → 0°). Indeed, for **CF−CF** and **POF−POF**, $\Delta\mu_{ge}$ varies between 0.37 and 1.58 D and between 0.54 and 1.47 D as a function of the conformation of the linker (Tables S16 and S18). In the next paragraph, we present the first hyperpolarizability values for the different compounds in each of their three states and we see that these can be rationalized, to a given extent, by using the linear optical responses.

3.4. Nonlinear Optical Properties. The key second-order NLO properties of the DiBOX compounds, evaluated at the TDDFT/M06-2X/6-311+G(d)/IEF-PCM (acetonitrile) level of approximation, are listed in Table 3. For all the three DiBOX derivatives, to act as efficient NLO switches, the three different states should present very distinct β_{HRS}. For a large range of wavelengths, calculations reveal that the smallest β_{HRS}

https://doi.org/10.1021/acs.jpcb.1c01962
J. Phys. Chem. B 2021, 125, 3918−3931

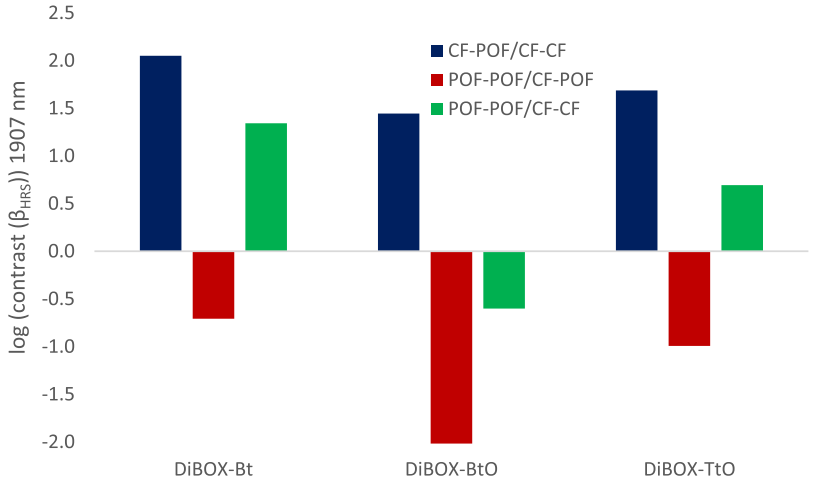

Figure 5. Effect of the linker on the β_{HRS} contrasts for an incident wavelength of 1907 nm, as calculated at the TDDFT/M06-2X/6-311+G(d)/IEF-PCM (acetonitrile) level of approximation.

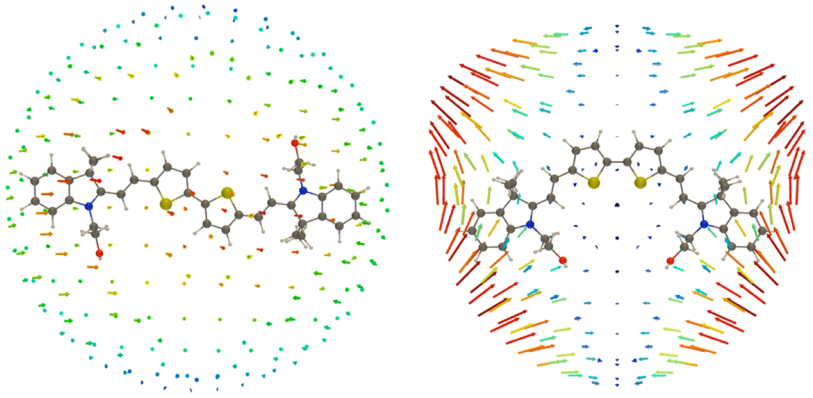

Figure 6. Progressive increase in the static β response of DiBOX-Bt in **POF−POF** upon the C_i-like → C_{2v}-like change of symmetry. Left: conformer 1 ($\beta_{HRS} < 0.1 \times 10^3$ a.u.) and right: conformer 2 ($\beta_{HRS} = 13 \times 10^3$ a.u., DR = 2.31). A USR factor of 1×10^{-4} (5) Å a.u.$^{-1}$ was used for conformer 2 (1).

values are achieved with the fully closed forms, where the EWG potential of the BOX unit is not expressed. The first BOX opening, leading to **CF−POF** from **CF−CF**, induces a substantial increase in β_{HRS}, at least by a factor of 30 but often by 2 orders of magnitude. In this form exhibiting the largest $\Delta\mu_{ge}$, the second smallest ΔE_{ge} (yet close to the smallest one), and the smallest local BLAs, all systems present logically the largest β_{HRS} value. In the **CF−POF** state, they present a dipolar characteristic regardless of the nature of the π-conjugated linker and a depolarization ratio (DR) close to 5 [DR = 4.79 (DiBOX-Bt), 4.67 (DiBOX-BtO), and 4.84 (DiBOX-TtO)].

The second BOX opening leading to **POF−POF** from **CF−POF** generates a β_{HRS} decrease. As explained above, due to the (partial) centrosymmetry, the EWG characteristics of the indoleninium groups cancel each other, which prevent the systems to exhibit larger β_{HRS} responses. This is especially the case of DiBOX-BtO where the *syn* form of the bis-EDOT linker has a vanishingly small MB weight (*vide infra*), resulting in a contrast ratio around 0.01 for the **CF−POF** to **POF−POF** transition (at λ = 1300 nm). On the other hand, in DiBOX-Bt, the Λ-shape structures are more stable (steric interactions between the thiophene groups are smaller than those between the EDOTs), and in DiBOX-TtO, the Λ-shape structures are naturally present owing to the EDOT-thiophene-EDOT structure of the linker, conducting to observe smaller contrast ratios, 0.14 and 0.12, respectively (again at λ = 1300 nm). The comparison of the β_{HRS} contrasts of the three DiBOXs is summarized in Figure 5.

While the **CF−POF** species present a strong dipolar characteristic ($|\beta_{J=1}|$ larger than $|\beta_{J=3}|$ and $\rho < 1$) in all cases, the dipolar/octupolar characteristic of the other forms (**CF−CF** and **POF−POF**) depends on the nature of the linker. For DiBOX-Bt, for which the linker can be centrosymmetric or not (in the latter case, when the bithiophene adopts a *syn* conformation, the molecule can adopt a C_{2v}-like symmetry), the DR amounts to 3.54 and 3.74 for **CF−CF** and **POF−POF**, respectively. These values correspond to a slight predominance of the octupolar characteristic ($\rho \sim 1.2$). In both cases, this is due to the fact that some of the contributing conformers have a Λ-shape structure (DR around 3) while others have a 1-D NLO-phore characteristic (DR close to 5). As discussed in sub-section II.C, the change of conformation of bithiophene from *anti* to *syn* results in an increase in $\Delta\mu_{ge}$. Since within the TSA, β is directly proportional to $\Delta\mu_{ge}$, the β response of DiBOX-Bt increases upon *anti* to *syn* switching, as illustrated in Figure 6 for **POF−POF** using the unit sphere representation.[34]

When bithiophene is replaced by a bis-EDOT moiety as the π-conjugated linker, the *syn* conformation is impeded due to the steric hindrance between the two EDOT units. As a consequence, the **POF−POF** state of DiBOX-BtO exhibits a

https://doi.org/10.1021/acs.jpcb.1c01962
J. Phys. Chem. B 2021, 125, 3918−3931

very small β response, but we can also notice a significantly smaller DR than in DiBOX-Bt (2.26 *vs* 3.76), "translating" an enhancement of the octupolar characteristic of the system. An antagonist effect is observed on the **CF−CF** state, though the β responses are small. Under this state, DiBOX-BtO exhibits a more pronounced dipolar characteristic translated by a DR close to 5 than DiBOX-Bt (3.74). This is explained by the existence for **CF−CF** state of non-centrosymmetric conformers with non-negligible MB weights.

Last, the **CF−CF** and **POF−POF** states of DiBOX-TtO have ρ values equal to 0.92 and 1.83, respectively. These values are similar to their analogues of DiBOX-BtO (0.82 and 2.20), but not necessarily for the same reasons. Indeed, many conformers contribute to the MB population of the **CF−CF** state and larger β_{HRS} responses are associated with DR values close to 5, that is, typical of 1-D NLO-phores (conformers 5, 6, 12, 14, and 15, Table S25). Then, for the fully open species, no matter whether both θ_3 and θ_4 correspond to a *anti* conformation (~180°) or only one, the octupolar characteristic is always dominant ($1.8 < \rho < 2.1$). Therefore, for DiBOX-Bt with the bithiophene in *syn* conformation and DiBOX-TtO with *trans* conformations of the thiophene-EDOT units, the **POF−POF** state corresponds to Λ-shaped **A−D−A** (attractor-donor-attractor) NLO-phores, with larger β responses than in DiBOX-BtO. In order to enhance the β responses of the **POF−POF** form, several strategies can be foreseen to constrain the conformation of the linker so that the EWGs draw a Λ-shape form. This can be achieved by using rigid linkers or, like in the present study, by combining an odd number of aromatic units adopting an *anti* conformation (DiBOX-TtO) or an even number of aromatic units allowing *syn* conformation (DiBOX-Bt).

The DiBOX-BT results were confronted to experimental data at 1300 nm (Table 3). For **CF−POF**, the computational and the experimental procedures give responses of the same order of magnitude (77×10^3 a.u. *vs* 88×10^3 a.u., respectively). On the other hand, the computations underestimate strongly the responses of **CF−CF** and **POF−POF**. This leads to a general overestimation of the β_{HRS} contrasts. Nevertheless, as illustrated in Figure 7, the experimental trends are reproduced. Yet, as discussed in the Methods section, measurements were only made for DiBOX-Bt because we did not succeed in synthesizing DiBOX-BtO, while HRS measurements on DiBOX-TtO were hampered by a huge two-photon fluorescence.

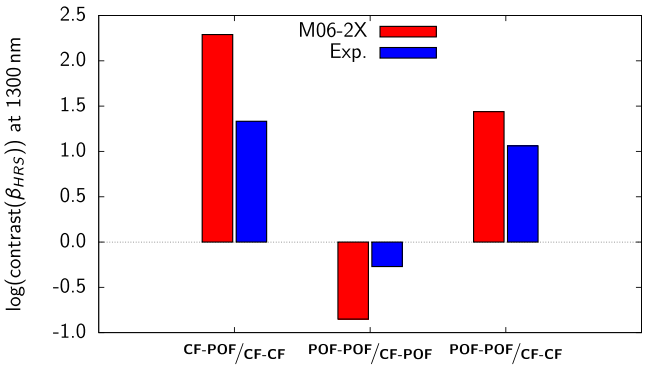

Figure 7. Contrasts of the β_{HRS} responses for the individual opening reactions of DiBOX-Bt as well as for the whole switching from the fully closed to the fully open forms, as represented by their log[contrast (β_{HRS})] at 1300 nm. The experimental results are compared to the calculations enacted at the TDDFT/M06-2X/6-311+G(d)/IEF-PCM (acetonitrile) level of theory.

4. FURTHER DISCUSSION, CONCLUSIONS, AND OUTLOOK

By adopting a multi-disciplinary approach that combines synthesis, UV/vis absorption, and hyper-Rayleigh scattering measurements together with quantum chemical calculations performed at the DFT level, it has been shown that DiBOX derivatives possessing two identical BOX units are efficient NLO switches. Since each BOX can be either closed or open, these systems can adopt three different states (**CF−CF**, **CF−POF**, and **POF−POF**). In these compounds, the acceptor characteristic of the BOX units is unleashed when it opens to form an indoleninium unit, so that low excitation energies are obtained for the **CF−POF** and **POF−POF** states. Then, since non-centrosymmetry is required to achieve non-zero first hyperpolarizability, only the non-symmetric **CF−POF** state is expected to exhibit a substantial β response. Indeed, calculations show that the β(**CF−POF**)/β(**CF−CF**) contrast is larger than 10, corresponding to the opening of the first BOX, while β(**POF−POF**)/β(**CF−POF**) is smaller than 1/3 for the opening of the second. Still, these contrasts depend on the nature of the linker, which controls not only the extent of the π-electron delocalization but also the symmetry of the system. In particular, better contrasts are achieved when centrosymmetry can be enforced for the fully open and fully closed states, in other words, when these two states have zero or negligible first hyperpolarizabilities. From the DFT analysis, it is shown that such centrosymmetry can be enforced when the linker between the BOXs contains two EDOT units (in the case of the DiBOX-BtO compound) because they can adopt a *anti* centrosymmetric conformation while the *syn* conformation is prevented due to steric hindrance. On the other hand, when the central part of the linker is replaced by a bithiophene (DiBOX-Bt compound), there is a non-zero population of the *syn* conformation. Similarly, when the linker is an EDOT−thiophene−EDOT sequence, a Λ-shape conformation is the most stable, leading to β responses that are not negligible—though still smaller—with respect to those of the corresponding **CF−POF** state. Beyond this static or stationary picture of the compounds, there are vibrational motions that can lift these pseudo-symmetries and lead to additional contributions to the β_{HRS} responses, like the so-called zero-point vibrational average responses.

Calculations provide further evidence that the largest β_{HRS} responses (in the **CF−POF** state) are achieved with the largest linker, EDOT−thiophene−EDOT, owing to better push−pull π-delocalization effects, as shown by the largest $\Delta\mu_{ge}$ among the three DiBOXs (Table 2). Taking advantage of the TSA[33] where $\beta \propto f_{ge}\Delta\mu_{ge}/\Delta E_{ge}{}^3$ and assuming a dominant 1D characteristic for the static first hyperpolarizability, the following relationship holds

$$\beta_{HRS} = \sqrt{\frac{6}{35}}\beta_{zzz} = 3.73\frac{f_{ge}\Delta\mu_{ge}}{\Delta E_{ge}{}^3}$$

Then, using the MB averages of Table 2, the corresponding TSA static β_{HRS} values of the **CF−POF** state of DiBOX-Bt, DiBOX-BtO, and DiBOX-TtO amount to 35×10^3, 30×10^3, and 82×10^3 a.u., respectively. These values match well with the full static β_{HRS} values given in Table 3.

https://doi.org/10.1021/acs.jpcb.1c01962
J. Phys. Chem. B 2021, 125, 3918−3931

To complement the experimental investigations of the successive switching steps, which can operate by the addition of acid or of oxidant, and therefore to analyze the control of the level of opening of these molecules, the Gibbs free energies were calculated for the following reactions (298.15 K in acetonitrile; the most stable conformer of each state was considered)

$$\text{CF–CF} + \text{HA} \rightarrow \text{CF–POF} + \text{A}^-[\Delta G^0(1)]$$

$$\text{CF–POF} + \text{HA} \rightarrow \text{POF–POF} + \text{A}^-[\Delta G^0(2)]$$

where HA is an acid and A^- is its conjugate base. Besides the irreversibility of the reactions [ΔG^0(**1** and/or **2**) < 0], in particular we concentrated on their difference, [$\Delta\Delta G^0 = \Delta G^0(\mathbf{2}) - \Delta G^0(\mathbf{1})$], because a negative value would mean that the second opening is easier than the first one and therefore that the level of opening cannot be controlled, which would be in contradiction with experiment. For DiBOX-Bt, using the M06 XC functional, the 6-311G(d) basis set and IEF-PCM, positive $\Delta G^0(\mathbf{1})$ values of 61 and 31 kJ mol^{-1} were calculated when HA is acetic acid and formic acid, demonstrating that these are poor acids to trigger the transformation, respectively. On the other hand, with $HClO_4$ $\Delta G^0(\mathbf{1})$ amounts to −81 and to −15 kJ mol^{-1} for trifluoroacetic acid (TFA), the acid that is often employed experimentally. We then considered only TFA as the acid and found that the opening reaction is facilitated in the case of DiBOX-BtO [$\Delta G^0(\mathbf{1}) = -59$ kJ mol^{-1}] and DiBOX-TtO [$\Delta G^0(\mathbf{1}) = -50$ kJ mol^{-1}]. Finally, calculations were performed, for DiBOX-Bt, at the ωB97X-D/6-311+G(d)/IEF-PCM level, and it was found that the second opening is less favorable [$\Delta G^0(\mathbf{2}) = -10$ kJ mol^{-1}] than the first [$\Delta G^0(\mathbf{1}) = -24$ kJ mol^{-1}] so that $\Delta\Delta G^0 = 14$ kJ mol^{-1}.

The opening by oxidation was then investigated (also by considering the most stable conformers). It consists of four steps (Scheme S2): (i) oxidation of the CF to form a radical cation, (ii) the C–O bond breaking (homolytic cleavage), (iii) the reduction of the product, and (iv) its protonation to obtain the POF. The rate-determining step is the first one (Table S28) so that the potential of oxidation *versus* the Fc/Fc^+ electrode (ferrocene/ferrocenium system) was evaluated. In the case of DiBOX-Bt, M06/6-311G(d)/IEF-PCM calculations predict that the oxidation potential amounts to 0.34 V for the **CF–CF** state, while for **CF–POF**, it amounts to 0.71 V. This larger value is attributed to the fact that it is more difficult to extract an electron from **CF–POF**, which bears a positive charge. In the case of DiBOX-BtO, the successive redox potentials *versus* the Fc/Fc^+ electrode amount to −0.12 and 0.39 V, evidencing the role of the better electron-donating bis-EDOT with respect to bithiophene. These redox potentials further decrease in the case of the EDOT–thiophene–EDOT linker with values of −0.18 and 0.18 eV, highlighting now the role of a larger π-conjugated linker. Therefore, owing to the fact that the redox potentials are larger for the second opening and that they are sufficiently different (differences of 0.51 V for DiBOX-BtO, 0.37 V for DiBOX-Bt, and 0.36 V for DiBOX-TtO), the calculations also demonstrate that the level of opening can also be controlled by redox reactions. These results also provide evidence that this computational protocol can be employed to other, not yet synthesized, compounds in the process of designing new multi-state switches with a control of its successive transformations. The analysis of the spin density distribution of the oxidized species (Figure S2) and the related atomic spin densities (Table S29) demonstrates that it is delocalized over the π-linker with large values on the vinyl C atom adjacent to the BOX unit (named C_{BOX}, Scheme S3). This atom is directly involved in the cleavage step and its larger atomic spin density in **CF–POF$^{+\bullet}$** than in **CF–CF$^{+\bullet}$** accounts for the fact that the cleavage is less endergonic for the second opening than the first (Table S28). Calculations further show that these C_{BOX} spin densities are similar for DiBOX-BtO but smaller for DiBOX-TtO, where the spin density is delocalized over three rings rather than two.

The general good agreement between the calculations on DiBOX derivatives and experiment demonstrates that the same approach can be used to study other multi-state multi-addressable BOX derivatives and therefore to help selecting the best ones for the synthesis. The current directions of investigation encompass the study of (i) DiBOX with asymmetric linkers and (ii) TriBOX and TetraBOX derivatives with symmetric or asymmetric linkers in order to improve the control of the switching process as well as to maximize the linear and nonlinear optical property contrasts. Different functionalization patterns can also be investigated.[35] Among these, the use of linkers able to chelate transition metals would open the field considerably.[36−38] Though it does not affect the design strategy, from the methodological and computational viewpoint, it is important to explain why the predicted β_{HRS} values of the **CF–CF** and **POF–POF** states of DiBOX-Bt are underestimated with respect to experiment. This could require using sequential molecular dynamics and then quantum chemistry approaches as done recently for ion pairs and chromophores embedded in lipid bilayers.[39,40]

■ ASSOCIATED CONTENT

Supporting Information

The Supporting Information is available free of charge at https://pubs.acs.org/doi/10.1021/acs.jpcb.1c01962.

Details (in particular the whole list of conformers, enabling the evaluation of the averages given in the manuscript) on optimized geometries and Maxwell–Boltzmann distribution, UV/vis absorption spectra and related quantities, nonlinear optical properties, redox reactions, details on the synthesis, HRS measurements, and UV/vis absorption spectra and the related properties (PDF)

■ AUTHOR INFORMATION

Corresponding Authors

Vincent Rodriguez − *Institut des Sciences Moléculaires (ISM, UMR CNRS 5255), Université de Bordeaux, 33405 Talence, France;* orcid.org/0000-0001-6804-9757; Email: vincent.rodriguez@u-bordeaux.fr

Lionel Sanguinet − *Univ Angers, CNRS, MOLTECH—Anjou, F-49000 Angers, France;* orcid.org/0000-0002-4334-9937; Email: lionel.sanguinet@univ-angers.fr

Benoît Champagne − *Theoretical Chemistry Laboratory, Unit of Theoretical and Structural Physical Chemistry, Namur Institute of Structured Matter, University of Namur, B-5000 Namur, Belgium;* orcid.org/0000-0003-3678-8875; Email: benoit.champagne@unamur.be

Authors

Jean Quertinmont − *Theoretical Chemistry Laboratory, Unit of Theoretical and Structural Physical Chemistry, Namur*

https://doi.org/10.1021/acs.jpcb.1c01962
J. Phys. Chem. B 2021, 125, 3918−3931

Institute of Structured Matter, University of Namur, B-5000 Namur, Belgium; orcid.org/0000-0001-9408-1451

Pierre Beaujean − *Theoretical Chemistry Laboratory, Unit of Theoretical and Structural Physical Chemistry, Namur Institute of Structured Matter, University of Namur, B-5000 Namur, Belgium*

Julien Stiennon − *Theoretical Chemistry Laboratory, Unit of Theoretical and Structural Physical Chemistry, Namur Institute of Structured Matter, University of Namur, B-5000 Namur, Belgium*

Youssef Aidibi − *Univ Angers, CNRS, MOLTECH—Anjou, F-49000 Angers, France*

Philippe Leriche − *Univ Angers, CNRS, MOLTECH—Anjou, F-49000 Angers, France*

Complete contact information is available at: https://pubs.acs.org/10.1021/acs.jpcb.1c01962

Notes

The authors declare no competing financial interest.

■ ACKNOWLEDGMENTS

J.Q. thanks the "Actions de Recherche Concertées" (ARC) de la Direction générale de l'Enseignement non obligatoire et de la Recherche scientifique—Direction de la Recherche scientifique—Communauté française de Belgique under convention no. 15/20-068 for his PhD grant. This work, carried out within the MORIARTY project, has benefited from the financial support from Wallonie-Bruxelles International (WBI), from the Fund for Scientific Research (F.R.S.-FNRS), from the French Ministry of Foreign and European Affairs, and from the Ministry of Higher Education and Research in the frame of the Hubert Curien partnerships. V.R. is grateful to F. Adamietz for experimental support and technical developments and also thanks the Région Nouvelle Aquitaine for financial support (CRA: 2015-1R10205-00004858). This work has been partly done in the frame of "the Investments for the future" Programme IdEx Bordeaux—LAPHIA (ANR-10-IDEX-03-02). The calculations were performed on the computers of the Consortium des Équipements de Calcul Intensif (CÉCI, http://www.ceci-hpc.be) and particularly those of the Technological Platform of High-Performance Computing, for which the authors gratefully acknowledge the financial support of the FNRS-FRFC, of the Walloon Region, and of the University of Namur (convention nos. 2.5020.11, GEQ U.G006.15, 1610468, and RW/GEQ2016), as well as on zenobe, the Tier-1 facility of the Walloon Region (convention 1117545).

■ REFERENCES

(1) Bissell, R. A.; Córdova, E.; Kaifer, A. E.; Stoddart, J. F. A Chemically and Electrochemically Switchable Molecular Shuttle. *Nature* **1994**, *369*, 133−137.

(2) de Silva, A. P.; Vance, T. P.; West, M. E. S.; Wright, G. D. Bright Molecules with Sense, Logic, Numeracy and Utility. *Org. Biomol. Chem.* **2008**, *6*, 2468−2480.

(3) Feringa, B. L.; Browne, W. R. *Molecular Switches*, 2nd ed.; Wiley-VCH: Weinheim, 2011.

(4) Andréasson, J.; Pischel, U. Molecules with a Sense of Logic: a Progress Report. *Chem. Soc. Rev.* **2015**, *44*, 1053−1069.

(5) Muller, P. Glossary of terms used in physical organic chemistry (IUPAC Recommendations 1994). *Pure Appl. Chem.* **1994**, *66*, 1077−1184.

(6) Bamfield, P.; Hutchings, M. G. Phenomena Involving a Stimulated Colour Change. *Chromic Phenomena: Technological Applications of Colour Chemistry*, 2 ed.; Royal Society of Chemistry, 2010; Chapter 1, pp 9−140.

(7) Kassem, S.; van Leeuwen, T.; Lubbe, A. S.; Wilson, M. R.; Feringa, B. L.; Leigh, D. A. Artificial Molecular Motors. *Chem. Soc. Rev.* **2017**, *46*, 2592−2621.

(8) McConnell, A. J.; Wood, C. S.; Neelakandan, P. P.; Nitschke, J. R. Stimuli-Responsive Metal-Ligand Assemblies. *Chem. Rev.* **2015**, *115*, 7729−7793.

(9) Coe, B. J. Molecular Materials Possessing Switchable Quadratic Nonlinear Optical Properties. *Chem.—Eur. J.* **1999**, *5*, 2464−2471.

(10) Delaire, J. A.; Nakatani, K. Linear and Nonlinear Optical Properties of Photochromic Molecules and Materials. *Chem. Rev.* **2000**, *100*, 1817−1846.

(11) Castet, F.; Rodriguez, V.; Pozzo, J.-L.; Ducasse, L.; Plaquet, A.; Champagne, B. Design and Characterization of Molecular Nonlinear Optical Switches. *Acc. Chem. Res.* **2013**, *46*, 2656−2665.

(12) Mançois, F.; Sanguinet, L.; Pozzo, J.-L.; Guillaume, M.; Champagne, B.; Rodriguez, V.; Adamietz, F.; Ducasse, L.; Castet, F. Acido-Triggered Nonlinear Optical Switches: Benzazolo-Oxazolidines. *J. Phys. Chem. B* **2007**, *111*, 9795−9802.

(13) Mançois, F.; Pozzo, J.-L.; Pan, J.; Adamietz, F.; Rodriguez, V.; Ducasse, L.; Castet, F.; Plaquet, A.; Champagne, B. Two-Way Molecular Switches with Large Nonlinear Optical Contrast. *Chem.—Eur. J.* **2009**, *15*, 2560−2571.

(14) Pielak, K.; Bondu, F.; Sanguinet, L.; Rodriguez, V.; Champagne, B.; Castet, F. Second-Order Nonlinear Optical Properties of Multiaddressable Indolinooxazolidine Derivatives: Joint Computational and Hyper-Rayleigh Scattering Investigations. *J. Phys. Chem. C* **2017**, *121*, 1851−1860.

(15) Szaloki, G.; Sanguinet, L. Properties and Applications of Indolinooxazolidines as Photo-, Electro- and Acidochromic Units. In: *Photon-Working Switches*, 1st ed; Yokoyama, Y., Nakatani, K., Eds.; Springer Japan, 2017; pp 69−93.

(16) Sanguinet, L.; Pozzo, J.-L.; Rodriguez, V.; Adamietz, F.; Castet, F.; Ducasse, L.; Champagne, B. Acido- and Phototriggered NLO Properties Enhancement. *J. Phys. Chem. B* **2005**, *109*, 11139−11150.

(17) Bondu, F.; Hadji, R.; Szalóki, G.; Alévêque, O.; Sanguinet, L.; Pozzo, J.-L.; Cavagnat, D.; Buffeteau, T.; Rodriguez, V. Huge Electro-/Photo-/Acidoinduced Second-Order Nonlinear Contrasts From Multiaddressable Indolinooxazolodine. *J. Phys. Chem. B* **2015**, *119*, 6758−6765.

(18) Hadji, R.; Szalóki, G.; Alévêque, O.; Levillain, E.; Sanguinet, L. The Stepwise Oxidation of Indolino[2,1-b]oxazolidine Derivatives. *J. Electroanal. Chem.* **2015**, *749*, 1−9.

(19) Szalóki, G.; Alévêque, O.; Pozzo, J.-L.; Hadji, R.; Levillain, E.; Sanguinet, L. Indolinooxazolidine: a Versatile Switchable Unit. *J. Phys. Chem. B* **2015**, *119*, 307−315.

(20) Houbrechts, S.; Clays, K.; Persoons, A.; Pikramenou, Z.; Lehn, J.-M. Hyper-Rayleigh Scattering Investigation of Nitrobenzyl Pyridine Model Compounds for Optical Modulation of the Hyperpolarisability. *Chem. Phys. Lett.* **1996**, *258*, 485−489.

(21) Beaujean, P.; Bondu, F.; Plaquet, A.; Garcia-Amorós, J.; Cusido, J.; Raymo, F. M.; Castet, F.; Rodriguez, V.; Champagne, B. Oxazines: A New Class of Second-Order Nonlinear Optical Switches. *J. Am. Chem. Soc.* **2016**, *138*, 5052−5062.

(22) Sevez, G.; Gan, J.; Delbaere, S.; Vermeersch, G.; Sanguinet, L.; Levillain, E.; Pozzo, J.-L. Photochromic Performance of a Dithienylethene-Indolinooxazolidine Hybrid. *Photochem. Photobiol.* **2010**, *9*, 131−135.

(23) Szalóki, G.; Sevez, G.; Berthet, J.; Pozzo, J.-L.; Delbaere, S. A simple Molecule-Based Octastate Switch. *J. Am. Chem. Soc.* **2014**, *136*, 13510−13513.

(24) Bondu, F.; Quertinmont, J.; Rodriguez, V.; Pozzo, J.-L.; Plaquet, A.; Champagne, B.; Castet, F. Second-Order Nonlinear Optical Properties of a Dithienylethene-Indolinooxazolidine Hybrid: a Joint Experimental and Theoretical Investigation. *Chem.—Eur. J.* **2015**, *21*, 18749−18757.

(25) Sanguinet, L.; Berthet, J.; Szalóki, G.; Alévêque, O.; Pozzo, J.-L.; Delbaere, S. 13 Metastable States Arising from a Simple

Multifunctional Unimolecular System. *Dyes Pigments* **2017**, *137*, 490−498.
(26) Aidibi, Y.; Guerrin, C.; Alévêque, O.; Leriche, P.; Delbaere, S.; Sanguinet, L. BT-2-BOX: An Assembly toward Multimodal and Multilevel Molecular System Simple as a Breeze. *J. Phys. Chem. C* **2019**, *123*, 11823−11832.
(27) Guerrin, C.; Aidibi, Y.; Sanguinet, L.; Leriche, P.; Aloise, S.; Orio, M.; Delbaere, S. When Light and Acid Play Tic-Tac-Toe with a Nine-State Molecular Switch. *J. Am. Chem. Soc.* **2019**, *141*, 19151−19160.
(28) Szalóki, G.; Sanguinet, L. Silica-Mediated Synthesis of Indolinooxazolidine-Based Molecular Switches. *J. Org. Chem.* **2015**, *80*, 3949−3956.
(29) Leriche, P.; Turbiez, M.; Monroche, V.; Frère, P.; Blanchard, P.; Skabara, P. J.; Roncali, J. Strong π-electron donors based on a self-rigidified 2,2′-bi(3,4-ethylenedioxy)thiophene-tetrathiafulvalene hybrid π-conjugated system. *Tetrahedron Lett.* **2003**, *44*, 649−652.
(30) Imae, I.; Sagawa, H.; Mashima, T.; Komaguchi, K.; Ooyama, Y.; Harima, Y. Synthesis of Soluble Polythiophene Partially Containing 3,4-Ethylenedioxythiophene and 3-Hexylthiophene by Polycondensation. *Open J. Polym. Chem.* **2014**, *04*, 83−93.
(31) Blanchard, P.; Cravino, A.; Levillain, E. Electrochemistry of Oligothiophenes and Polythiophenes. *Handbook of Thiophene-Based Materials*; John Wiley & Sons, Ltd, 2009; pp 419−453.
(32) Chevallier, F.; Charlot, M.; Mongin, F.; Champagne, B.; Franz, E.; Clays, K.; Blanchard-Desce, M. Synthetic, Optical and Theoretical Study of Alternating Ethylenedioxythiophene-Pyridine Oligomers: Evolution from Planar Conjugated to Helicoidal Structure Towards A Chiral Configuration. *ChemPhysChem* **2016**, *17*, 4090−4101.
(33) Oudar, J. L.; Chemla, D. S. Hyperpolarizabilities of the Nitroanilines and Their Relations to the Excited State Dipole Moment. *J. Chem. Phys.* **1977**, *66*, 2664−2668.
(34) Tuer, A.; Krouglov, S.; Cisek, R.; Tokarz, D.; Barzda, V. Three-Dimensional Visualization of the First Hyperpolarizability Tensor. *J. Comput. Chem.* **2011**, *32*, 1128−1134.
(35) Bureš, F. Fundamental Aspects of Property Tuning in Push-Pull Molecules. *RSC Adv.* **2014**, *4*, 58826−58851.
(36) Yam, V. W.-W.; Ko, C.-C.; Zhu, N. Photochromic and Luminescence Switching Properties of A Versatile Diarylethene-Containing 1,10-Phenanthroline Ligand and its Rhenium(I) Complex. *J. Am. Chem. Soc.* **2004**, *126*, 12734−12735.
(37) Guerchais, V.; Ordronneau, L.; Le Bozec, H. Recent Developments in the Field of Metal Complexes Containing Photochromic Ligands: Modulation of Linear and Nonlinear Optical Properties. *Coord. Chem. Rev.* **2010**, *254*, 2533−2545.
(38) Pielak, K.; Bondu, F.; Sanguinet, L.; Rodriguez, V.; Castet, F.; Champagne, B. Acido-Triggered Switching of the Second-Order Nonlinear Optical Properties of a Ferrocenyl-Containing Indolino-Oxazolidine Derivative. *Dyes Pigments* **2019**, *160*, 641−646.
(39) Pielak, K.; Tonnelé, C.; Sanguinet, L.; Cariati, E.; Righetto, S.; Muccioli, L.; Castet, F.; Champagne, B. Dynamical Behavior and Second Harmonic Generation Responses in Acido-Triggered Molecular Switches. *J. Phys. Chem. C* **2018**, *122*, 26160−26168.
(40) Bouquiaux, C.; Tonnelé, C.; Castet, F.; Champagne, B. Second-Order Nonlinear Optical Properties of an Amphiphilic Dye Embedded in a Lipid Bilayer. A Combined Molecular Dynamics-Quantum Chemistry Study. *J. Phys. Chem. B* **2020**, *124*, 2101−2109.
(41) Verreault, D.; Moreno, K.; Merlet, É.; Adamietz, F.; Kauffmann, B.; Ferrand, Y.; Olivier, C.; Rodriguez, V. Hyper-Rayleigh Scattering as a New Chiroptical Method: Uncovering the Nonlinear Optical Activity of Aromatic Oligoamide Foldamers. *J. Am. Chem. Soc.* **2020**, *142*, 257−263.
(42) Rodriguez, V. Polarization-Resolved Third-Harmonic Scattering in Liquids. *J. Phys. Chem. C* **2017**, *121*, 8510−8514.
(43) Castet, F.; Bogdan, E.; Plaquet, A.; Ducasse, L.; Champagne, B.; Rodriguez, V. Reference molecules for nonlinear optics: A joint experimental and theoretical investigation. *J. Chem. Phys.* **2012**, *136*, 024506.
(44) Zhao, Y.; Truhlar, D. G. The M06 suite of density functionals for main group thermochemistry, thermochemical kinetics, noncovalent interactions, excited states, and transition elements: two new functionals and systematic testing of four M06-class functionals and 12 other functionals. *Theor. Chem. Acc.* **2008**, *120*, 215−241.
(45) Tomasi, J.; Mennucci, B.; Cammi, R. Quantum Mechanical Continuum Solvation Models. *Chem. Rev.* **2005**, *105*, 2999−3094.
(46) Jacquemin, D.; Femenias, A.; Chermette, H.; Ciofini, I.; Adamo, C.; André, J.-M.; Perpète, E. A. Assessment of Several Hybrid DFT Functionals for the Evaluation of Bond Length Alternation of Increasingly Long Oligomers. *J. Phys. Chem. A* **2006**, *110*, 5952−5959.
(47) Scalmani, G.; Frisch, M. J.; Mennucci, B.; Tomasi, J.; Cammi, R.; Barone, V. Geometries and Properties of Excited States in the Gas Phase and in Solution: Theory and Application of a Time-Dependent Density Functional Theory Polarizable Continuum Model. *J. Chem. Phys.* **2006**, *124*, 094107.
(48) Le Bahers, T.; Adamo, C.; Ciofini, I. A Qualitative Index of Spatial Extent in Charge-Transfer Excitations. *J. Chem. Theory Comput.* **2011**, *7*, 2498−2506.
(49) van Gisbergen, S. J. A.; Snijders, J. G.; Baerends, E. J. Calculating Frequency-Dependent Hyperpolarizabilities Using Time-Dependent Density Functional Theory. *J. Chem. Phys.* **1998**, *109*, 10644−10656.
(50) Helgaker, T.; Coriani, S.; Jørgensen, P.; Kristensen, K.; Olsen, J.; Ruud, K. Recent Advances in Wave Function-Based Methods of Molecular-Property Calculations. *Chem. Rev.* **2012**, *112*, 543−631.
(51) Verbiest, T.; Clays, K.; Rodriguez, V. *Second-Order Nonlinear Optical Characterizations Techniques: an Introduction*; CRC Press: New York, 2009.
(52) Bersohn, R.; Pao, Y. H.; Frisch, H. L. Double-Quantum Light Scattering by Molecules. *J. Chem. Phys.* **1966**, *45*, 3184−3198.
(53) Brasselet, S.; Zyss, J. Multipolar Molecules and Multipolar Fields: Probing and Controlling the Tensorial Nature of Nonlinear Molecular Media. *J. Opt. Soc. Am. B* **1998**, *15*, 257−288.
(54) Rodriguez, V.; Grondin, J.; Adamietz, F.; Danten, Y. Local Structure in Ionic Liquids Investigated by Hyper-Rayleigh Scattering. *J. Phys. Chem. B* **2010**, *114*, 15057−15065.
(55) Liégeois, V., UNamur. DrawMol, www.unamur.be/drawmol (accessed on March 2021).
(56) Shelton, D. P.; Rice, J. E. Measurements and Calculations of the Hyperpolarizabilities of Atoms and Small Molecules in the Gas Phase. *Chem. Rev.* **1994**, *94*, 3−29.
(57) de Wergifosse, M.; Champagne, B. Electron correlation effects on the first hyperpolarizability of push-pull π-conjugated systems. *J. Chem. Phys.* **2011**, *134*, 074113.
(58) Johnson, L. E.; Dalton, L. R.; Robinson, B. H. Optimizing Calculations of Electronic Excitations and Relative Hyperpolarizabilities of Electrooptic Chromophores. *Acc. Chem. Res.* **2014**, *47*, 3258−3265.
(59) Garrett, K.; Sosa Vazquez, X.; Egri, S. B.; Wilmer, J.; Johnson, L. E.; Robinson, B. H.; Isborn, C. M. Optimum Exchange for Calculation of Excitation Energies and Hyperpolarizabilities of Organic Electro-Optic Chromophores. *J. Chem. Theory Comput.* **2014**, *10*, 3821−3831.
(60) Champagne, B.; Beaujean, P.; de Wergifosse, M.; Cardenuto, M.; Liégeois, V.; Castet, F. *Frontiers of Quantum Chemistry*; Wojcik, M., Nakatsuji, H., Kirtman, B., Ozaki, Y., Eds.; Springer: Singapore, 2018, pp 117−138.
(61) Lescos, L.; Sitkiewicz, S. P.; Beaujean, P.; Blanchard-Desce, M.; Champagne, B.; Matito, E.; Castet, F. Performance of DFT Functionals for Calculating the Second-Order Nonlinear Optical Properties of Dipolar Merocyanines. *Phys. Chem. Chem. Phys.* **2020**, *22*, 16579−16594.
(62) Frisch, M.; Trucks, G.; Schlegel, H.; Scuseria, G.; Robb, M.; Cheeseman, J.; Scalmani, G.; Barone, V.; Mennucci, B.; Petersson, G. et al. *Gaussian 16* Rev. A.03; Gaussian Inc.: Wallingford CT, 2016.

https://doi.org/10.1021/acs.jpcb.1c01962
J. Phys. Chem. B 2021, 125, 3918−3931